LOCAL DEGRADATION AND DAMAGE INDUCED BY THERMO-OXIDATION IN CARBON-EPOXY COMPOSITE MATERIALS

M. Gigliotti*, D. Q. Vu, M. C. Lafarie-Frenot

[1]*Institute Pprime – CNRS – ENSMA - Université de Poitiers*
Département de Physique et Mécanique des Matériaux
1, Avenue Clément Ader, F86961, Futuroscope Chasseneuil Cedex, FRANCE
**e-mail: marco.gigliotti@ensma.fr*
Tel: +33(0)549498340
Fax: +33(0)549498238

Keywords: Thermo-oxydation, confocal interferometric microscopy, matrix shrinkage, fibre/matrix debonding.

Abstract

The present paper is concerned with thermo-oxidative-induced degradation and damage in carbon-epoxy composite materials at the microscopic scale. Confocal Interferometric Microscopy (CIM) measures and Scanning Electronic Microscope (SEM) observations have been carried out on IM7/977-2 composite UD samples aged under atmospheric air at 150°C, showing the occurrence of matrix shrinkage – whose extent depends on conditioning time and fibre-to-fibre spacing - and fibre/matrix debonding, after around 1000h conditioning. By comparison with experimental observation, a numerical model simulating thermo-oxidative-induced matrix shrinkage and stress can be employed to estimate the critical energy release rate for fibre/matrix debonding.

1 Introduction

Composite materials possess very interesting specific mechanical properties (strength and stiffness) and very good fatigue resistance and are today largely employed within aircraft/aerospace structures. To be employed in structural parts subjected to rather severe thermal conditions (for instance, composite structures for aero – engines) their behaviour at moderate and high temperatures must be characterised: under such conditions thermo-oxidation reaction/diffusion phenomena take place within the polymer material eventually inducing degradation and damage. Thermo-oxidation of organic matrix composites has been the subject of specific studies over the past ten years [1-4] mainly focusing on the resin material alone: the coupled oxygen diffusion/reaction phenomenon leads to matrix chemical shrinkage strains and to the development of an oxidised layer in which the mechanical properties of the material are degraded. At the microscopic scale (the scale of the fibre), the coupling between stress concentration close to the fibre/matrix interfaces and thermo-oxidative matrix degradation can lead to microscopic damage, such as fibre/matrix debonding. The present paper is concerned with thermo-oxidative-induced degradation and damage in carbon-epoxy composite materials at the microscopic scale. Confocal Interferometric

Microscopy (CIM) measures and Scanning Electronic Microscope (SEM) observations have been carried out on IM7/977-2 composite UD samples aged under atmospheric air at 150°C, showing the occurrence of matrix shrinkage – whose extent depends on conditioning time and fibre-to-fibre spacing - and fibre/matrix debonding, after around 1000h conditioning. By comparison with experimental observation, a numerical model simulating thermo-oxidative-induced matrix shrinkage and stress can be employed to estimate the critical energy release rate for fibre/matrix debonding.

2 Testing methods and experimental measurements

Composite samples were oxidised for 192 h and 1000 h at 150°C under atmospheric air in dedicated climatic chambers opportunely conceived for such applications. Figure 1 shows a view of this setup and some details of the sample fixation system.

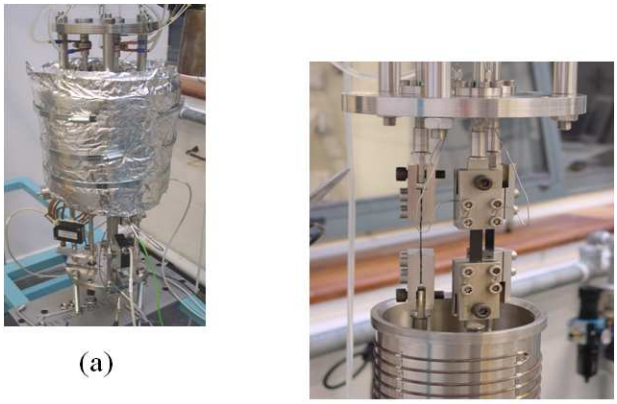

Figure 1. View of the climatic chambers (a) and some details of the sample fixation system (b)

Thermo-oxidative-induced shrinkage profiles have been measured on the side surfaces of CFRP IM7/977-2 carbon-epoxy samples cut from thick $[0]_{40}$ UD composite plates by Confocal Interferometric Microscopy (CIM), by employing a Taylor Hobson TALYSURF CCI 6000 microscope, whose measure technique is based on Michelson interferometry; with a 50x magnification, this apparatus is able to extract 3D images and profiles with a vertical resolution up to 10^{-5} µm along a 0.35 x 0.35 mm^2 surface. Values of slopes higher than 27° cannot be measured by the apparatus and are reported as unmeasured points (NM). Figure 2 illustrates a typical image (observed at room temperature) captured by the apparatus at the side surface edges (exposed to the environment) of an oxidised composite sample, aged at 150°C.

The illustration shows the presence of matrix and fibre rich zones within the composite and possibly a certain amount of unmeasured points. By analogy with Scanning Electron Microscopy (SEM) clichés the unmeasured points can be correlated to matrix microcracks, flaws and fibre/matrix debondings. From 3D cartographies, thermo-oxidation-induced shrinkage profiles can be extracted: moreover, by zooming on the zone of interest (Fig. 2), matrix shrinkage profiles between two fibres can be measured and the corresponding maximal shrinkage depth can be quantified. Interrupted tests can be also carried out: the experimental setup allows re-finding the same thermo-oxidised zones and following the evolution of the shrinkage profiles.

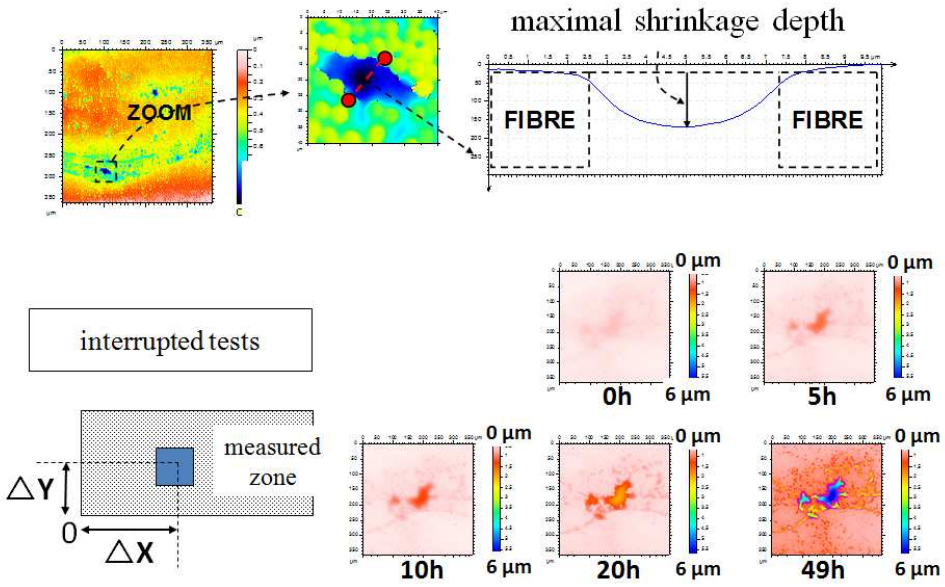

Figure 2. Example of images extracted by CIM at the exposed side edge surfaces of an oxidised composite sample and measurement of thermo-oxidative-induced shrinkage profiles

Thermo-oxidative-induced matrix shrinkage can be therefore qualitatively and quantitatively characterised as a function of the fibre-to-fibre distance by extracting and post-processing a certain number of profiles such as that illustrated in Fig. 2. Additional details about the experimental technique can be found in references [3] and [4].

3 Modelling of thermo-oxidation and polymer mechanical behaviour

The composite can be modelled as a two-phase material characterised by the fibres, which are thermally and chemically stable with respect to oxidation, and by the polymer material in which the ageing process takes place. The fibre/matrix interfaces are not modelled. The model is developed within the framework of the Thermodynamics of Irreversible Processes (TIP) (see, for instance, [5]) following a deterministic approach and with little use of phenomenological relationships. The chemical processes taking place during thermo-oxidation are detailed by a mechanistic scheme developed by Colin et al. [1], which allows predicting the evolution of each chemical species locally and at each instant of time during the thermo-oxidation process, taking into account reaction-diffusion couplings. The local evolution of the oxygen concentration within the polymer (noted $[O_2]$), due to both chemical reaction and species diffusion can be therefore determined by employing the mechanistic scheme by Colin et al. [1]: for more details about the mathematical representation of such scheme and its appropriate boundary conditions the reader is referred to references [1, 4]. Oxygen reaction-diffusion is normally characterised by a global parameter, the concentration of oxidation products, Q, defined by:

$$Q(x, y, z, t) = \int_0^t \frac{d[O_2]}{d\tau} d\tau \qquad (1)$$

The thermo-oxidative-induced shrinkage free strain tensor can be calculated starting from the knowledge of the advancement of the chemical reaction and is given by [6]:

$$\mathbf{E}^{\mathbf{SH}} = \frac{1}{3}\left(\frac{\Delta m}{m} - \frac{\Delta \rho}{\rho_0}\right)\mathbf{I}, \quad \frac{1}{m_0}\frac{dm}{dt} = \frac{1}{\rho_0}\left(M_{O2}\frac{d[O_2]}{dt} - M_{H2O}\frac{d[H_2O]}{dt} - M_v\frac{d[V]}{dt}\right) \tag{2}$$

where **I** is the identity tensor, m and ρ respectively the mass and the density of the material at time t, the index "0" indicates the same variables at the start time, and M_X the molar mass of the component X. The mechanical behaviour of the polymer material can be modelled by a nonlinear viscoelastic constitutive law, similar to that proposed by Cunat [7]:

$$\mathrm{Tr}\,\mathbf{S} = 3K_V\,\mathrm{tr}\,\mathbf{E} - 3K_V\,\mathbf{E}^{TH} - 3K_V\,\mathbf{E}^{\mathbf{SH}} - 3\sum_{j=1}^{n} K_j\, z_j^{\mathbf{trE}}$$

$$\mathbf{S^d} = 2G_V\,\mathbf{E^d} - 2\sum_{j=1}^{m} G_j\,\mathbf{Z}_j^{\mathbf{Ed}} \tag{3}$$

with:

$$K_j = p_j^{K}\,K_R \text{ and } G_j = p_j^{G}\,G_R$$
$$\sum_{j=1}^{n} p_j^{K} = 1 \text{ and } \sum_{j=1}^{m} p_j^{G} = 1 \tag{4}$$

in which **S** is the stress tensor, **E** the strain tensor, the index "d" refers to the deviatoric part of the corresponding tensor and $\mathbf{E}^{TH}$ is the free thermal strain tensor: in this model, the "j" internal variables, which rule the viscoelastic behaviour, are noted by $z_j^{\mathbf{trE}}$ and $\mathbf{Z}_j^{\mathbf{Ed}}$ (for the spherical and the deviatoric part, respectively). The model uses fifty variables, each with its own relaxation time, $\tau_j^{\mathbf{trE}}$ and $\tau_j^{\mathbf{Ed}}$, respectively. The weights p_j^{K} and p_j^{G} of the distribution associated to each characteristic time follow a law similar to that proposed by Cunat [7]. The internal variables are ruled by differential equations of the type:

$$\frac{d\,z_j^{\mathbf{trE}}}{dt} = \frac{1}{a_s(T)\tau_j^{\mathbf{trE}}}\left(z_j^{\mathbf{trE}} - z_\infty^{\mathbf{trE}}\right)$$
$$\frac{d\,\mathbf{Z}_j^{\mathbf{Ed}}}{dt} = \frac{1}{a_d(T)\tau_j^{\mathbf{Ed}}}\left(\mathbf{Z}_j^{\mathbf{Ed}} - \mathbf{Z}_\infty^{\mathbf{Ed}}\right) \tag{5}$$

The parameters of the model are: the glass and relaxed moduli of the resin, K_V, K_R, G_V, G_R, a coefficient of the distribution law (not detailed here) and the functions $a_s(T)$ et $a_d(T)$. The model has been identified by relaxation traction tests at 150°C performed on unoxidised pure resin samples. In this model, thermo mechanics couplings are represented by the free thermal strain tensor term depending on the free expansion of the resin and by the functions $a_s(T)$ and $a_d(T)$. Chemo mechanics couplings are taken into account by the thermo oxidation induced shrinkage strain tensor, $\mathbf{E}^{SH}$, calculated by Eq. 2. The model integrates also the expression of the local indentation modulus (EIT) of the resin as a function of the concentration of oxygen products, Eq. 1, identified by Ultra Micro Indentation (UMI) tests. The model has been implemented into the ABAQUS finite element commercial code [9] via the available user subroutines. More details about the model and its numerical implementation can be found in references [4] and [8].

4 Results and discussion

Figure 3 shows the measured maximal shrinkage depth as a function of the fibre-to-fibre distance for samples aged 192 h and 1000 h under atmospheric air at 150°C and SEM clichés of the observed external surfaces.

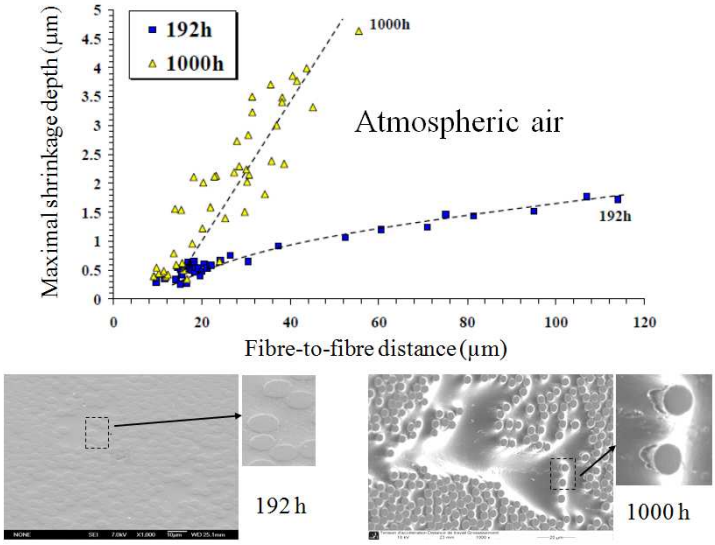

Figure 3. Maximal shrinkage depth as a function of the fibre-to-fibre distance for samples aged under atmospheric air, at 150°C for 192 h and 1000 h and SEM clichés of the observed surfaces

For both samples, the maximal shrinkage depth increases for increasing fibre-to-fibre distance, its magnitude being higher for the 1000 h thermo-oxidised sample. SEM observations show that the 192 h aged sample surface presents some matrix shrinkage while the 1000 h aged sample surface exhibits matrix shrinkage and fibre/matrix debonding at some interfaces.

Figure 4 shows the experimental and the numerically simulated thermo-oxidative-induced matrix shrinkage (maximal depth and profiles between fibres) for samples aged under atmospheric air, at 150°C for 192 h and 1000 h.

A good agreement is obtained for 192 h aged samples: for 1000 h aged samples both maximal shrinkage and profile predictions are far from the measured ones. This is due to the occurrence of fibre/matrix debonding at the interface as it is proved by SEM observation and by direct profile measurement (the presence of non-measured points close to some interfaces, see Fig. 4).

Figure 5 shows experimental vs. numerically simulated thermo-oxidation-induced matrix shrinkage for samples aged under atmospheric air, at 150°C 1000 h. Calculations are performed including fibre/matrix debonding of variable depth, h, at the interfaces.

It can be noted that – for the 1000 h aged sample - the agreement between the experimental and the numerically simulated matrix shrinkage can be increased by adding fibre/matrix debonding at the interfaces. Moreover, increasing the fibre-to-fibre distance, the fibre/matrix debonding depth must be increased for a correct simulation of the thermo-oxidative-induced shrinkage.

In fact, for a 20 µm fibre-to-fibre distance, the fibre/matrix debonding depth is around 10 µm while, for a 40 µm fibre-to-fibre distance, the fibre/matrix debonding depth is around 30 µm.

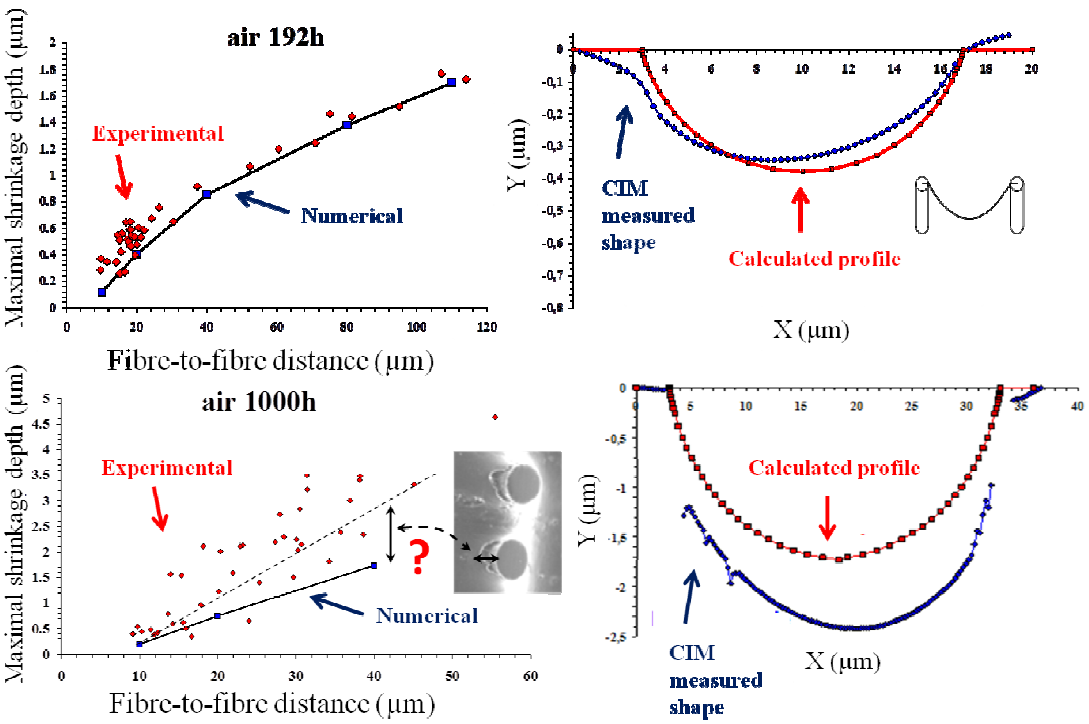

Figure 4. Experimental vs. numerically simulated thermo-oxidative-induced matrix shrinkage (maximal depth and profiles between fibres) for samples aged under atmospheric air, at 150°C for 192 h and 1000 h

This tendency indicated that higher fibre-to-fibre distances – related to matrix rich zones and low local fibre volume fraction values – tend to develop more damage: this conclusion is qualitatively supported by experimental observation (mainly SEM observation), though it is difficult to measure fibre/matrix debonding depth with a good level of precision.

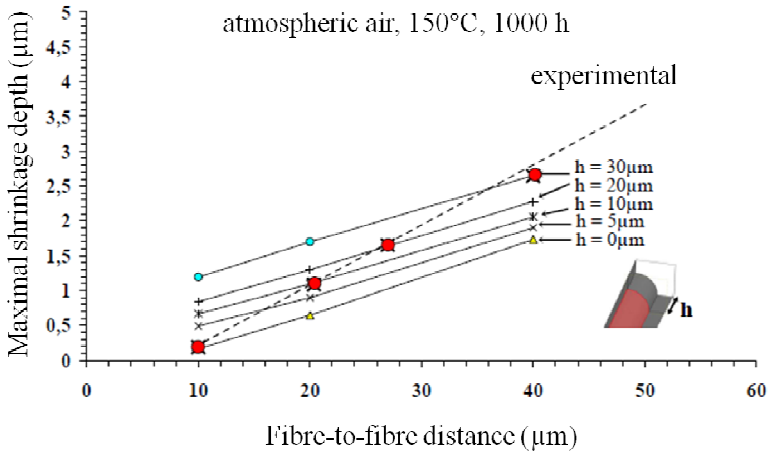

Figure 5. Experimental vs. numerically simulated thermo-oxidative-induced matrix shrinkage for samples aged under atmospheric air, at 150°C 1000 h. Calculations are performed including fibre/matrix debonding (of variable depth, h) at the interfaces

By employing the numerical model, the energy release rate related to the onset of fibre/matrix debonding at the interface can be estimated for a given fibre/matrix debonding depth by the formula:

$$G_d = -\frac{\Delta E}{\Delta A} \quad (6)$$

For h approaching zero, this calculation approaches the value of energy release rate for the onset of debonding. More details can be found in reference [4]
Figure 6 illustrates the calculated values of G_d as a function of the fibre-to-fibre distance, for samples aged under atmospheric air, at 150°C 1000 h.

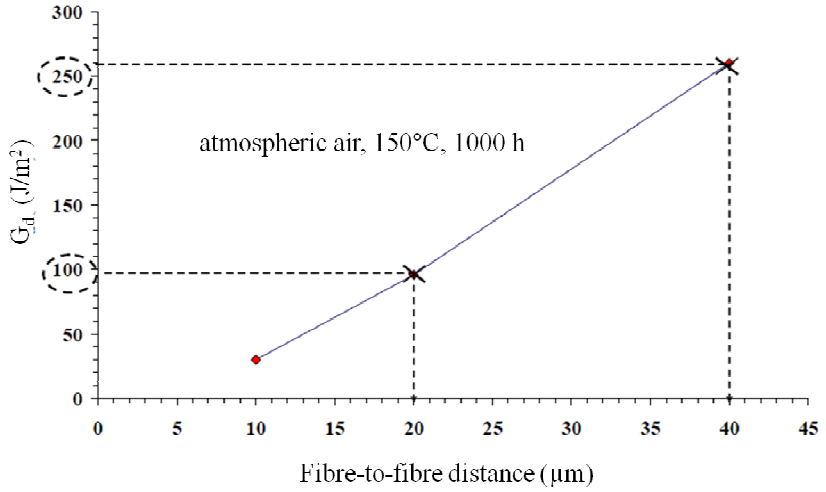

Figure 6. Calculated values of the energy release rate for fibre/matrix debonding onset, G_d, as a function of the fibre-to-fibre distance, for samples aged under atmospheric air, at 150°C 1000 h.

It can be noted that G_d increases by increasing the fibre-to-fibre distance. This again indicates that zones with higher fibre-to-fibre distances tend to develop more damage in the form of fibre/matrix debonding, if one assumes that this form of damage occurs when the calculated G_d equals a critical energy release rate value, G_{dc}. The exact identification of G_{dc} is difficult since, for a 1000 h aging time, for instance, we are not able to detect exactly a configuration (an interface) in which fibre/matrix debonding is at the onset. However, if we limit ourselves to fibre-to-fibre distances between 20 µm and 40 µm – which have already developed some damage – the identified value of G_{dc} is between 100 and 250 J/m^2.

5 Conclusions

Confocal Interferometric Microscopy (CIM) measures and Scanning Electronic Microscope (SEM) observations have been carried out on IM7/977-2 composite UD samples aged under atmospheric air at 150°C, showing the occurrence of matrix shrinkage – whose extent depends on conditioning time and fibre-to-fibre spacing - and fibre/matrix debonding, after around 1000h conditioning. By comparison with experimental observation, a numerical model simulating thermo-oxidative-induced matrix shrinkage and stress has been employed to estimate the critical energy release rate for fibre/matrix debonding.

Acknowledgments

We would like to thank Dr. Jacques Cinquin (EADS IW, Suresnes) for providing the IM7/977-2 composite material under study.

References

[1] Colin X., Marais C., Verdu J. A New Method for Predicting the Thermal Oxidation of Thermoset Matrices. Application to an Amine Crosslinked Epoxy. *Polymer Testing*, **20**, pp. 795-803 (2001).

[2] Pochiraju K.V., Tandon G.P., Shoeppner G.A. Evolution of stress and Deformations in High-Temperature Polymer Matrix Composites During Thermo-Oxidative Aging. *Mechanics of Time Dependent Materials*, **12**, pp. 45-68 (2008).

[3] Vu D.Q., Gigliotti M., Lafarie-Frenot M.C. Experimental Characterization of Thermo-Oxidation-Induced Shrinkage and Damage in Polymer-Matrix Composites. *Composites Part A: Applied Science and Manufacturing*, **43**, pp. 577-586 (2012).

[4] Vu, D.Q. Endommagements induits par la thermo oxydation dans les composites carbone/epoxy unidirectionnels et stratifiés. *PhD Thesis, University of Poitiers - Ecole Nationale Supérieure de Mécanique et d'Aérotechnique* (ENSMA): Poitiers – France, 2011. Published by Editions Universitaires Européennes, ISBN : 978-3-8417-8925-9 (2011).

[5] Kondepoudi D., Prigogine, I. Modern Thermodynamics: from Heat Engines to Dissipative Structures. *Wiley, New York* (1998).

[6] Decelle J., Huet N., Bellenger V. Oxidation Induced Shrinkage for Thermally Aged Epoxy Networks. *Polymer Degradation and Stability*, **81**, pp. 239-248 (2003).

[7] Cunat C. The DLNR Approach and Relaxation Phenomena. Part I: Historical Account and DLNR Formalism. *Mechanics of Time Dependent Materials*, **5**, pp. 39-65. (2001).

[8] Gigliotti M., Olivier L., Vu D.Q., Grandidier J.C., Lafarie-Frenot M.C. Local Shrinkage and Stress Induced by Thermo-Oxidation in Composite Materials at High Temperatures. *Journal of the Mechanics and Physics of Solids*, **59**, pp. 696-712 (2011).

[9] SIMULIA ABAQUS FEM Software, Ver. 6.7, Users Manual.